ALX1 induces Snail expression to promote epithelial to mesenchymal transition and invasion of ovarian cancer cells

Hong Yuan[1], Hiroaki Kajiyama[1], Satoko Ito[2], Nobuhisa Yoshikawa[1], Toshinori Hyodo[2], Eri Asano[2], Hitoki Hasegawa[2], Masao Maeda[2], Kiyofumi Shibata[1] Michinari Hamaguchi[2], Fumitaka Kikkawa[1], Takeshi Senga[2]

[1]Department of Obstetrics and Gynecology, Nagoya University Graduate School of Medicine, 65 Tsurumai, Showa, Nagoya, 466-8550, Japan

[2]Division of Cancer Biology, Nagoya University Graduate School of Medicine, 65 Tsurumai, Showa, Nagoya, 466-8550, Japan

Running title: ALX1 regulates EMT

Address correspondence to:

Hiroaki Kajiyama M.D., Ph.D.; 65 Tsurumai-cho, Showa-ku, Nagoya, 466-8550, Japan

Phone: 81-52-744-2262; Fax: 81-52-744-2268; E-mail: kajiyama@med.nagoya-u.ac.jp

Takeshi Senga M.D., Ph.D.; 65 Tsurumai-cho, Showa-ku, Nagoya, 466-8550, Japan

Phone: 81-52-744-2463; Fax: 81-52-744-2464; E-mail: tsenga@med.nagoya-u.ac.jp

Keywords: ALX1, Snail, EMT, Ovarian cancer, invasion

Conflict of interest: The authors report no conflicts of interest.

Word count: 6383

Total number of figures: 6

Abstract

Ovarian cancer is a highly invasive and metastatic disease with a poor prognosis if diagnosed at an advanced stage, which is often the case. Recent studies argue that ovarian cancer cells that have undergone epithelial to mesenchymal transition (EMT) acquire aggressive malignant properties, but the relevant molecular mechanisms in this setting are not well understood. Here we report findings from an siRNA screen that identified the homeobox transcription factor ALX1 as a novel regulator of EMT. RNAi-mediated attenuation of ALX1 expression restored E-cadherin expression and cell-cell junction formation in ovarian cancer cells, suppressing cell invasion, anchorage-independent growth and tumor formation. Conversely, enforced expression of ALX1 in ovarian cancer cells or non-tumorigenic epithelial cells induced EMT. We found that ALX1 upregulated expression of the key EMT regulator Snail (SNAI1) and that it mediated EMT activation and cell invasion by ALX1. Our results define the ALX1/Snail axis as a novel EMT pathway that mediates cancer invasion.

Introduction

Ovarian cancer is a highly metastatic disease and the most lethal of the gynecologic malignancies. Despite advances in cytotoxic therapies for numerous types of cancer, the current therapies available to ovarian cancer patients in advanced stages have little effect, as evidenced by the poor 5-yr survival rate (1,2). To provide insight that will enable the development of new therapeutic strategies, it is crucial to elucidate the molecular mechanisms that promote the invasive and metastatic properties of ovarian cancer cells. Recent studies have demonstrated that a morphologic conversion, known as epithelial to mesenchymal transition (EMT), is associated with the acquisition of malignant characteristics in ovarian cancer cells (3-8).

EMT is a complex multi-step process that occurs during embryonic development, tumor progression, and tissue fibrosis (9,10). During EMT, epithelial cells lose many of their epithelial characteristics and adopt a mesenchymal appearance and mesenchymal characteristics, such as increased motility and invasiveness. Dynamic changes in gene expression and cytoskeletal re-organization are often observed during the process of EMT (11). One of the hallmarks of EMT is the suppression of E-cadherin, a transmembrane protein essential for cell-cell adhesions. The loss of E-cadherin expression not only disrupts cell-cell adhesion but also activates multiple pathways that induce cellular dissemination, invasion and metastasis (12).

Extensive studies have revealed that EMT is governed by a variety of regulatory networks. EMT is triggered by extracellular stimuli, such as transforming growth factor β (TGF-β), fibroblast growth factor (FGF), hepatocyte growth factor (HGF) and endothelin-1 (ET-1) (13,14). The signaling pathways activated by these factors induce changes in cytoskeletal organization and disrupt cell-cell junctions. In addition to these

signaling pathways, transcription factors, such as Snail, Slug, Twist, Zeb1 and SIP1, have been found to play crucial roles in promoting EMT (15). Among them, Snail is the most extensively studied and has been associated with tumor progression (16). Snail is a zinc-finger transcription factor that binds to E-box sequences located in the promoter regions of target genes (17,18). Snail can also regulate transcription by modifying local chromosomal structures via the recruitment of histone deacetylase 1 (HDAC1) and HDAC2, as well as the co-repressor Sin3A (19). In addition to the well-known EMT inducers, recent studies have unveiled novel EMT-related transcription factors, such as HOXB7 (20), SIX1 (21,22), FOXQ1 (23,24), and FOXM1 (25). These findings indicate that EMT is regulated by a diverse set of transcription factors. Thus, the identification of additional factors will give further insight into the molecular mechanisms regulating EMT.

To search for novel regulators of EMT, we performed a limited siRNA screen and found that Aristaless-like homeobox1 (ALX1), also known as Cart1 (26,27), is important for the induction of morphological changes in ovarian cancer cells. Previous studies have shown that ALX1 is required for neuronal or craniofacial development (28,29), but the detailed physiological role of ALX1 remains largely unknown. In this report, we demonstrate that ALX1 induces EMT and cell invasion in ovarian cancer cells by promoting Snail expression.

Materials and Methods

Materials and Methods have also been described in Supplementary Materials.

Cells, antibodies and chemicals

All the ovarian cancer cells were cultured in RPMI supplemented with 10% FBS and antibiotics. K1, K2, NOS3, NOS4, TTOV and TAOV cells were established in the Department of Obstetrics and Gynecology, Nagoya University Graduate School of Medicine (30). ES-2 and RMG-II cells are originated from clear cell carcinoma and other cell lines are from serous carcinoma. 293T cells were maintained in DMEM supplemented with 10% FBS with antibiotics. MCF10A cells were obtained from ATCC and maintained in DMEM-F12 supplemented with 0.1 μg/ml cholera toxin (Sigma, St. Louis, MO), 0.02 μg/ml epidermal growth factor (PeproTech, Rocky Hill, NJ), 10 μg/ml insulin (Sigma), 0.5 μg/ml hydrocortisone (Sigma), 100 U/ml penicillin, 100 μg/ml streptomycin, and 5% horse serum (Invitrogen, Carlsbad, CA). Antibodies were obtained from the following companies: Anti-E-cadherin, anti-N-cadherin, anti-vimentin antibodies, BD Biosciences, San Jose, CA; anti-β-actin, anti-vinculin antibodies, Sigma; anti-GFP antibody, Neuro Mab, Davis, CA; anti-Snail antibodies, Cell Signaling, Danvers, MA. Rhodamine-conjugated phalloidin was obtained from Invitrogen and DAPI from Dojindo (Kumamoto, Japan).

Clinical samples for quantitative RT-PCR

Cancer tissues were obtained with informed consent and approval of the ethics committee of Nagoya University. Details of patients' samples are described in supplementary table 1.

siRNA screening

Transcription factors that exhibited increased expression in ovarian cancer were selected from data derived from experiments performed by Welsh et al. and Lancaster et

al. deposited in Oncomine (31-33). Forty-eight transcription factors were manually selected and 2 siRNAs targeting each gene were transfected to SKOV3 cells cultured in 24-well plates. Seventy-two hour later, cells were fixed and stained with rhodamine-conjugated phalloidin. Pictures were taken and morphological changes were evaluated by 2 independent researchers.

Luciferase assay

The previously reported promoter region for Snail (-1558/+92) (34) was amplified and cloned into the pGL4 vector (Promega). 293T cells were transfected with the pGL4-Snail/promoter together with pQCXIP-GFP-ALX1 and pRTK-Luc to normalize transfection efficiency. Forty-eight hours later, the activities of Firefly luciferase and Renilla luciferase were measured using the Dual Luciferase Reporter Assay System (Promega). Luciferase activity was measured in triplicate and three independent experiments were performed. To measure luciferase activity in the absence of ALX1 expression, SKOV3 cells were transfected with control or ALX1 siRNA together with pRTK-Luc and pGL4-Snail/promoter. Seventy-two hours later, luciferase activities were measured.

Statistical analysis

Statistical analysis for cell invasion, colony formation, and tumor formation in mice was performed using Student's t-test. $P<0.05$ was considered statistically significant. The association between ALX1 expression and tumor stage was determined by Chi-squared-test. The correlation between ALX1 and Snail expression, or ALX1 and Slug expression in cancer tissues was determined by Pearson's correlation coefficient.

Results

Depletion of ALX1 induces reversion of EMT

To search for novel transcription factors associated with EMT and aggressive characteristics in ovarian cancer cells, we performed a limited siRNA screen. We manually selected 48 transcription factors that were previously reported to exhibit increased expression in ovarian cancer (32,33). SKOV3 cells were transfected with siRNAs targeting these transcription factors and changes in cellular morphology were examined. We predicted that the depletion of genes relevant to EMT would induce an epithelial morphology with tight cell-cell adhesion in SKOV3 cells. In this screen, we discovered that the transfection of 2 different ALX1-targeting siRNAs induced morphological changes in SKOV3 cells. Thus, we decided to investigate roles for ALX1 in the induction of EMT and the acquisition of aggressive characteristics in ovarian cancer cells.

We first evaluated the expression levels of ALX1 mRNA in ovarian cancer cell lines using quantitative RT-PCR analysis. The expression of ALX1 mRNA was greatest in the ES-2, HEY and SKOV3 cells (Fig. 1A). Interestingly, the expression level of ALX1 mRNA was related with the malignant characteristics of ovarian cancer cells. ES-2, HEY and SKOV3 cells were more invasive than other ovarian cancer cell lines and were able to grow under anchorage-independent conditions (Fig. S1). To determine the expression of ALX1 in ovarian cancer, we performed in situ hybridization using tissue microarrays. We found that strong expression of ALX1 mRNA was observed in some cancer tissues, and the expression was correlated with tumor stage (Fig. 1B). We then examined the effects of ALX1 depletion in the cell lines with high ALX1 expression.

ALX1 depletion induced the recovery of cell-cell adhesions and the cellular morphology became more like that of epithelial cells (Fig. 1C). Immunostaining analysis revealed that knocking down ALX1 expression induced a clear recovery of E-cadherin localization in HEY and SKOV3 cells, but not in ES-2 cells (Fig. 1C). We speculated that the cells had undergone a reversion of EMT by ALX1 depletion in HEY and SKOV3 cells. To test this hypothesis, the expression levels of epithelial and mesenchymal markers were examined. ALX1 mRNA expression was sufficiently suppressed by both siRNAs (Fig. 1D). The up-regulation of E-cadherin and the down-regulation of N-cadherin and vimentin were detected at both the mRNA and the protein levels in HEY and SKOV3 cells (Fig. 1D and 1E). However, ES-2 cells did not show any changes in expression of these markers by ALX1 knockdown (Fig. 1D and 1E). We performed rescue experiment to exclude the possibility of off-target effects of siRNAs. SKOV3 cells that constitutively expressed GFP-ALX1 or siRNA-resistant GFP-ALX1 (ALX-Res#2) were established by retrovirus infection. ALX1 siRNA effectively ablated exogenously expressed wild-type GFP-ALX1, but not siRNA-resistant GFP-ALX1 (Fig. S2). Changes in expression of the marker proteins were not observed in cells that expressed siRNA-resistant GFP-ALX1 (Fig. S2). These results indicate that ALX1 is crucial for SKOV3 and HEY cells to maintain mesenchymal characteristics, but ES-2 cells may have additional factors that prevent cells from undergoing reversion of EMT by ALX1 depletion.

ALX1 regulates cell invasion and anchorage independent growth.

EMT is associated with malignant properties, such as invasion and anchorage-independent growth (35,36). We tested whether ALX1 was required for these properties in ovarian cancer cells. To assess cell invasiveness, we used Matrigel-coated

Boyden chambers. The invasion of HEY, SKOV3 and ES-2 cells was significantly suppressed by ALX1 knock-down (Fig. 2A). The reduced invasiveness by ALX1 depletion is not due to the impaired viability of cells because cell proliferation was not inhibited by ALX1 siRNA-transfection (Fig. S3). We next assessed anchorage-independent cell growth in the ALX1-depleted cells. As shown in figure 2B, the silencing of ALX1 expression suppressed colony formation in soft agar. To test whether the inhibition of ALX1 expression affected cancer cell growth in vivo, we generated SKOV3 cells that constitutively expressed shRNA targeting either luciferase (shCtrl) or ALX1 (shALX1). ALX1 mRNA was reduced and E-cadherin expression was induced in shALX1 cells (Fig. 2C). ShCtrl and shALX1 cells were subcutaneously injected to the femoral area of nude mice and tumor formation was examined. Both cell lines formed six subcutaneous tumors out of seven injected sites. The tumor formation of shALX1 cells was suppressed compared with the tumor formation of shCtrl cells (Fig. 2D). Mice were sacrificed 36 days after tumor cell injection and the tumor weight was determined. The average tumor weight of shALX1 cells was significantly reduced compared with that of shCtrl cells (Fig. 2E).

Exogenous expression of ALX1 confers malignant phenotype.

We next determined whether the exogenous expression of ALX1 confers a more malignant phenotype to ovarian cancer cells. In addition to a homeodomain in the central region of the protein, ALX1 has a conserved amino acid stretch known as the aristaless domain or OAR domain (Fig. 3A). We generated SKOV3 cells that constitutively expressed GFP (GFP), GFP-tagged full-length ALX1 (FL), or GFP-tagged ALX1 lacking either the homeodomain (Δhomeo) or the OAR domain (ΔOAR). FL and

ΔOAR localized to the nucleus, but Δhomeo diffusely localized to both the cytoplasm and the nucleus (Fig. 3B). FL and ΔOAR SKOV3 cells exhibited more elongated and spindle-like shapes than the GFP and Δhomeo SKOV3 cells (Fig. 3B). The expression of E-cadherin was eliminated in FL and ΔOAR SKOV3 cells, but not in GFP and Δhomeo SKOV3 cells (Fig. 3C). In addition, the expression of N-cadherin and vimentin was up-regulated in FL and ΔOAR SKOV3 cells (Fig. 3C). We next assessed the effects of ALX1 expression on invasion and anchorage-independent growth. Both FL and ΔOAR SKOV3 cells were significantly more invasive than the GFP and Δhomeo SKOV3 cells (Fig. 3D). Furthermore, expression of FL and ΔOAR clearly promoted the anchorage-independent growth of SKOV3 cells (Fig. 3E). Promotion of EMT, anchorage-independent growth and invasion by ALX1 expression was also observed using additional ovarian cancer cell line, NOS3 (Fig. S4). These results demonstrate that ALX1 is associated with aggressive phenotype of ovarian cancer cells.

Exogenous expression of ALX1 in non-tumorigenic cells induces EMT

To further extend our analysis of the role of ALX1 in EMT, we determined whether ALX1 can induce EMT in non-tumorigenic epithelial cells. MCF10A cells are non-transformed mammary epithelial cells characterized by well-organized cell-cell junctions. We generated GFP, FL, Δhomeo, and ΔOAR MCF10A cells by retroviral infection. Both GFP and Δhomeo MCF10A cells maintained a cobblestone-like morphology that was similar to parental cells (Fig. 4A). In contrast, FL and ΔOAR MCF10A cells appeared elongated and the cell-cell junctions were disrupted (Fig. 4A). E-cadherin was localized along the cell-cell junctions in GFP and Δhomeo MCF10A cells, but was absent in FL and ΔOAR MCF10A cells (Fig. 4B). Remodeling of the actin

cytoskeleton is often observed during EMT. Both GFP and Δhomeo MCF10A cells primarily exhibited cortical F-actin formation along cell-cell junctions, whereas the clear organization of actin stress fibers across the cell was observed in the FL and ΔOAR MCF10A cells (Fig. 4C). Consistent with the observed changes in actin cytoskeleton organization, the formation of focal adhesions was evident in FL and ΔOAR MCF10A cells (Fig. 4C). ALX1-induced EMT was further confirmed by immunoblot analysis. FL and ΔOAR MCF10A cells exhibited a decrease in E-cadherin expression that was concomitant with an increase in the expression of both N-cadherin and vimentin (Fig. 4D). The expression of ALX1 also promoted migration and invasion of MCF10A cells (Fig. 4E and 4F).

ALX1 regulates Snail expression

To gain further insight into the molecular mechanisms by which ALX1 regulates EMT and malignant conversion, we aimed to identify transcription factors whose expression is regulated by ALX1. RNA was extracted from SKOV3, HEY and ES-2 cells that had been transfected with ALX1-targeting siRNA, and the mRNA expression of EMT-related transcription factors was examined by RT-PCR. Among the transcription factors examined, Snail mRNA was decreased by the knock-down of ALX1 in SKOV3 and HEY cells, but not in ES-2 cells (Fig. 5A). The reduced expression of Snail protein in HEY and SKOV3 cells transfected with ALX1 siRNA was verified by immunoblot (Fig. 5B). Snail was localized in the nucleus of SKOV3 cells that were transfected with control siRNA (Fig. 5C). ALX1 knock-down suppressed nuclear Snail expression, which was concomitant with an increase in E-cadherin expression along cell-cell junctions (Fig. 5C). We next determined whether the exogenous expression of ALX1 up-regulates Snail

expression in SKOV3 and MCF10A cells. Whole cell extracts of GFP, FL, Δhomeo, and ΔOAR cells were subjected to immunoblot analysis and Snail expression was detected. As shown in figure 5D, Snail expression was increased in FL and ΔOAR cells compared with GFP and Δhomeo cells. We also performed luciferase assays to determine whether Snail promoter activity was regulated by ALX1 expression. 293T cells were transiently co-transfected with full-length ALX1 and a reporter construct in which the human Snail promoter region was cloned upstream of firefly luciferase (pGL4-Snail/promoter). Exogenous expression of ALX1 increased Snail promoter activity approximately 3.3 fold (Fig. 5E). In addition, the transfection of ALX1 siRNA into SKOV3 cells decreased promoter activity 40-50% compared with that of luciferase siRNA (Fig. 5F). These results indicate that ALX1 induces the transcription of the Snail gene. Finally, we examined whether ALX1 expression was related with Snail expression in ovarian cancer. The expression levels of ALX1 and Snail mRNA were evaluated in 19 ovarian cancer tissues by quantitative RT-PCR. As shown in figure 5G, we observed a significant correlation between ALX1 and Snail expression. However, the expression of Slug, a homolog of Snail, did not correlate with ALX1 expression (Fig. 5G).

Snail is required for ALX1-mediated EMT and cell invasion

If Snail expression is crucial for the ALX1-mediated EMT, then depletion of Snail is expected to reverse the morphological changes induced by ALX1 expression. To test this possibility, MCF10A cells that constitutively expressed GFP-ALX1 were transfected with Snail siRNA and changes in the expression of EMT-related proteins were examined. Immunofluorescence analysis showed that Snail depletion clearly restored E-cadherin localization to the cell-cell junctions (Fig. 6A). The increase in E-cadherin expression

and the decrease in both N-cadherin and vimentin expression were confirmed by immunoblot analysis in Snail knock-down cells (Fig. 6B). We next examined whether Snail expression was critical for ALX1-mediated EMT and cell invasion in SKOV3 cells. Similar to the results obtained from MCF10A cells, silencing Snail expression in ALX1-expressing SKOV3 cells restored epithelial properties, as indicated by the increased expression of epithelial markers (Fig. 6C). In addition, the invasive phenotype of ALX1-expressing SKOV3 was suppressed by Snail knock-down (Fig. 6D).

To further confirm the requirement of Snail for ALX1-dependent EMT, we generated SKOV3 cells that constitutively expressed GFP-Snail and then examined the effects of ALX1 depletion. If a decrease in Snail is crucial for the reversion of EMT induced by ALX1 knock-down, then the exogenous expression of Snail should prevent the reversion of EMT. SKOV3 cells expressing GFP-Snail were transfected with either control or ALX1 siRNA and after 72 h, the protein expression of epithelial and mesenchymal markers was examined by immunoblot. Changes in the expression of these markers indicated that the exogenous expression of Snail further promoted EMT in SKOV3 cells (Fig. 6E). ALX1 depletion in GFP SKOV3 cells induced an increase in E-cadherin expression and a decrease in both N-cadherin and vimentin expression, whereas ALX1 depletion in GFP-Snail SKOV3 cells did not induce changes in the expression of these marker proteins (Fig. 6E). We next assessed the invasion of GFP-Snail SKOV3 cells in the absence of ALX1 expression. As shown in figure 6F, ALX1 depletion did not suppress invasion in GFP-Snail SKOV3 cells. These results indicate that the ALX1-mediated promotion of EMT and cell invasion is dependent on Snail expression.

Discussion

Accumulating evidence indicates that EMT-associated transcription factors confer cancer cells with malignant characteristics, such as invasion, metastasis, and resistance to chemotherapy (15). In this study, we determined that the exogenous expression of ALX1 in SKOV3 cells induced mesenchymal characteristics and promoted cell invasion and colony formation in soft agar. The depletion of ALX1 induced morphological changes and suppressed anchorage-independent growth and cell invasion in HEY, SKOV3 and ES-2 cells. In addition, clear reversion of EMT was observed by ALX1 depletion in HEY and SKOV3 cells. Furthermore, the silencing of ALX1 expression in SKOV3 cells significantly suppressed tumor formation in mice. Collectively, these results indicate that ALX1 contributes to the promotion of EMT and the acquisition of malignant characteristics in ovarian cancer cells. However, ALX1-mediated EMT appears to be dependent on the cellular context because ALX1-depletion did not induce reversion of EMT in ES-2 cells. We also found that Snail expression was positively regulated by ALX1. Depletion of Snail inhibited ALX-mediated EMT and cell invasion, indicating that the ALX1/Snail axis is a novel pathway that contributes to the malignant conversion of ovarian cancer cells. A previous immunohistochemical analysis of ovarian cancer tissue demonstrated that Snail expression was high in metastatic lesions and that Snail expression correlates with tumor stage (37). Interestingly, we found that the expression of Snail and ALX1 was correlated in ovarian cancer tissues. These results suggest that ALX1 may regulate Snail expression in ovarian cancer, thereby promoting malignant conversion. In addition to ovarian cancer, Snail expression is associated with a poor prognosis and the recurrence of other tumors (16); thus, ALX1 may promote tumor progression in cancers other than ovarian cancer.

The exogenous expression of ALX1 induced EMT not only in cancer cells but also in non-tumorigenic MCF10A mammary epithelial cells. The expression of ALX1 in MCF10A cells induced the expression of mesenchymal markers and the reorganization of the cytoskeleton, which are changes associated with EMT. The ability of ALX1 to induce EMT in non-tumorigenic epithelial cells suggests that ALX1 may possess crucial roles in promoting EMT during development. Homozygous deletion of ALX1 gene in humans is associated with the severe disruption of early craniofacial development (29). ALX1 knockout mice exhibit defective neural tube closure and limb girdle development (28,38). These studies clearly demonstrate that ALX1 plays an essential role in mammalian development, but how ALX1 controls embryonic development remains largely unknown. Recent studies have shown that ALX1 is part of a gene regulatory network that is required for the development of sea urchins (39). ALX1 regulates the expression of genes, such as Twist, that induce EMT in primary mesenchyme cells (40). Therefore, ALX1 may contribute to the induction of EMT during the mammalian development, thereby promoting limb girdle and craniofacial formation.

The expression of EMT-associated transcription factors is regulated by integrated and complicated regulatory systems. Previous studies have elucidated some of the upstream regulators of ALX1 expression during development. A heterodimer composed of Pbx1 and Emx2, both of which are homeoproteins, binds directly to the conserved upstream sequence of the ALX1 gene (41). During sea urchin development, the activation of β-catenin induces ALX1 expression (27), and the phosphorylation of the Ets1 transcription factor by MAPK signaling maintains ALX1 expression (39). These findings implicate the existence of multiple regulatory mechanisms to control ALX1 expression.

Further investigation may reveal that these transcription factors promote EMT and malignant conversion of cancer cells by regulating ALX1 expression.

In summary, we have identified ALX1 as a novel regulator of EMT and cell invasion. In addition, the induction of Snail expression was demonstrated to be critical for the ALX1-mediated promotion of EMT and cell invasion. ALX3 and ALX4 are both ALX1 homologues that are required for craniofacial development in humans (42, 43). Whether ALX3 and ALX4 are associated with EMT and cancer progression remains unknown. The elucidation of the cellular functions of these ALX family members will provide additional information that may greatly improve our understanding of the regulatory networks governing EMT and cancer progression.

Acknowledgments

We would like to thank the members of the Division of Cancer Biology for their helpful discussions. This research was funded by a grant from Takeda Science Foundation and the Ministry of Education, Culture, Sports, Science and Technology of Japan.

References

1. Naora H, Montell DJ. Ovarian cancer metastasis: integrating insights from disparate model organisms. Nat Rev Cancer 2005;5:355-66.
2. Edwards BK, Brown ML, Wingo PA, Howe HL, Ward E, Ries LA, Schrag D, Jamison PM, Jemal A, Wu XC, Friedman C, Harlan L, Warren J, Anderson RN, Pickle LW. Annual report to the nation on the status of cancer, 1975-2002, featuring population-based trends in cancer treatment. J Natl Cancer Inst 2005;97:1407-27.

3. Yoshida J, Horiuchi A, Kikuchi N, Hayashi A, Osada R, Ohira S, Shiozawa T, Konishi I. Changes in the expression of E-cadherin repressors, Snail, Slug, SIP1, and Twist, in the development and progression of ovarian carcinoma: the important role of Snail in ovarian tumorigenesis and progression. Med Mol Morphol 2009;42:82-91.
4. Ponnusamy MP, Lakshmanan I, Jain M, Das S, Chakraborty S, Dey P, Batra SK. MUC4 mucin-induced epithelial to mesenchymal transition: a novel mechanism for metastasis of human ovarian cancer cells. Oncogene. 2010;29:5741-54
5. Cao L, Shao M, Schilder J, Guise T, Mohammad KS, Matei D. Tissue transglutaminase links TGF-β, epithelial to mesenchymal transition and a stem cell phenotype in ovarian cancer. Oncogene 2012;31:2521-34.
6. Elloul S, Vaksman O, Stavnes HT, Trope CG, Davidson B, Reich R. Mesenchymal-to-epithelial transition determinants as characteristics of ovarian carcinoma effusions. Clin Exp Metastasis 2010;27:161-72.
7. Kajiyama H, Shibata K, Terauchi M, Yamashita M, Ino K, Nawa A, Kikkawa F. Chemoresistance to paclitaxel induces epithelial-mesenchymal transition and enhances metastatic potential for epithelial ovarian carcinoma cells. Int J Oncol 2007;31:277-83.
8. Ahmed N, Thompson EW, Quinn MA. Epithelial-mesenchymal interconversions in normal ovarian surface epithelium and ovarian carcinomas: an exception to the norm. J Cell Physiol. 2007;213:581-8.
9. Yang J, Weinberg RA. Epithelial-mesenchymal transition: at the crossroads of development and tumor metastasis. Dev Cell 2008;14:818-29.

10. Thiery JP, Acloque H, Huang RY, Nieto MA. Epithelial-mesenchymal transitions in development and disease. Cell 2009;139:871-90.
11. Yilmaz M, Christofori G. EMT, the cytoskeleton, and cancer cell invasion. Cancer Metastasis Rev 2009;28:15-33.
12. Onder TT, Gupta PB, Mani SA, Yang J, Lander ES, Weinberg RA. Loss of E-cadherin promotes metastasis via multiple downstream transcriptional pathways. Cancer Res 2008;68:3645-54.
13. Vergara D, Merlot B, Lucot JP, Collinet P, Vinatier D, Fournier I, Salzet M. Epithelial-mesenchymal transition in ovarian cancer. Cancer Lett. 2010;291:59-66.
14. Rosanò L, Spinella F, Di Castro V, Nicotra MR, Dedhar S, de Herreros AG, Natali PG,Bagnato A. Endothelin-1 promotes epithelial-to-mesenchymal transition in human ovarian cancer cells. Cancer Res 2005;65:11649-57.
15. Peinado H, Olmeda D, Cano A. Snail, Zeb and bHLH factors in tumour progression: an alliance against the epithelial phenotype? Nat Rev Cancer 2007;7:415-28.
16. Wu Y, Zhou BP. Snail: More than EMT. Cell Adh Migr 2010;4:199-203.
17. Batlle E, Sancho E, Francí C, Domínguez D, Monfar M, Baulida J, García De Herreros A. The transcription factor snail is a repressor of E-cadherin gene expression in epithelial tumour cells. Nat Cell Biol 2000;2:84-9.
18. Cano A, Pérez-Moreno MA, Rodrigo I, Locascio A, Blanco MJ, del Barrio MG, Portillo F, Nieto MA. The transcription factor snail controls epithelial-mesenchymal transitions by repressing E-cadherin expression. Nat Cell Biol. 2000;2:76-83.
19. Peinado H, Ballestar E, Esteller M, Cano A. Snail mediates E-cadherin repression by the recruitment of the Sin3A/histone deacetylase 1 (HDAC1)/HDAC2 complex. Mol Cell Biol 2004;24:306-19.

20. Wu X, Chen H, Parker B, Rubin E, Zhu T, Lee JS, Argani P, Sukumar S. HOXB7, a homeodomain protein, is overexpressed in breast cancer and confers epithelial-mesenchymal transition. Cancer Res 2006;66:9527-34.
21. Micalizzi DS, Christensen KL, Jedlicka P, Coletta RD, Barón AE, Harrell JC, Horwitz KB, Billheimer D, Heichman KA, Welm AL, Schiemann WP, Ford HL. The Six1 homeoprotein induces human mammary carcinoma cells to undergo epithelial-mesenchymal transition and metastasis in mice through increasing TGF-beta signaling. J Clin Invest 2009;119:2678-90.
22. McCoy EL, Iwanaga R, Jedlicka P, Abbey NS, Chodosh LA, Heichman KA, Welm AL, Ford HL. Six1 expands the mouse mammary epithelial stem/progenitor cell pool and induces mammary tumors that undergo epithelial-mesenchymal transition. J Clin Invest 2009;119:2663-77.
23. Zhang H, Meng F, Liu G, Zhang B, Zhu J, Wu F, Ethier SP, Miller F, Wu G. Forkhead transcription factor foxq1 promotes epithelial-mesenchymal transition and breast cancer metastasis. Cancer Res 2011;71:1292-301.
24. Qiao Y, Jiang X, Lee ST, Karuturi RK, Hooi SC, Yu Q. FOXQ1 regulates epithelial-mesenchymal transition in human cancers. Cancer Res 2011;71:3076-86.
25. Bao B, Wang Z, Ali S, Kong D, Banerjee S, Ahmad A, Li Y, Azmi AS, Miele L, Sarkar FH. Over-expression of FoxM1 leads to epithelial-mesenchymal transition and cancer stem cell phenotype in pancreatic cancer cells. J Cell Biochem 2011;112:2296-306.
26. Zhao GQ, Zhou X, Eberspaecher H, Solursh M, de Crombrugghe B. Cartilage homeoprotein 1, a homeoprotein selectively expressed in chondrocytes. Proc Natl Acad Sci U S A 1993;90:8633-7.

27. Ettensohn CA, Illies MR, Oliveri P, De Jong DL. Alx1, a member of the Cart1/Alx3/Alx4 subfamily of Paired-class homeodomain proteins, is an essential component of the gene network controlling skeletogenic fate specification in the sea urchin embryo. Development 2003;130:2917-28.

28. Zhao Q, Behringer RR, de Crombrugghe B. Prenatal folic acid treatment suppresses acrania and meroanencephaly in mice mutant for the Cart1 homeobox gene. Nat Genet 1996;13:275-83.

29. Uz E, Alanay Y, Aktas D, Vargel I, Gucer S, Tuncbilek G, von Eggeling F, Yilmaz E, Deren O, Posorski N, Ozdag H, Liehr T, Balci S, Alikasifoglu M, Wollnik B, Akarsu NA. Disruption of ALX1 causes extreme microphthalmia and severe facial clefting: expanding the spectrum of autosomal-recessive ALX-related frontonasal dysplasia. Am J Hum Genet 2010;86:789-96.

30. Kajiyama H, Kikkawa F, Suzuki T, Shibata K, Ino K, Mizutani S. Prolonged survival and decreased invasive activity attributable to dipeptidyl peptidase IV overexpression in ovarian carcinoma. Cancer Res 2002;62:2753-7.

31. Rhodes DR, Yu J, Shanker K, Deshpande N, Varambally R, Ghosh D, Barrette T, Pandey A, Chinnaiyan AM. ONCOMINE: a cancer microarray database and integrated data-mining platform. Neoplasia 2004;6:1-6.

32. Lancaster JM, Dressman HK, Whitaker RS, Havrilesky L, Gray J, Marks JR, Nevins JR, Berchuck A. Gene expression patterns that characterize advanced stage serous ovarian cancers. J Soc Gynecol Investig 2004;11:51-9.

33. Welsh JB, Sapinoso LM, Kern SG, Brown DA, Liu T, Bauskin AR, Ward RL, Hawkins NJ, Quinn DI, Russell PJ, Sutherland RL, Breit SN, Moskaluk CA, Frierson HF Jr, Hampton GM. Large-scale delineation of secreted protein

biomarkers overexpressed in cancer tissue and serum. Proc Natl Acad Sci U S A 2003;100:3410-5.

34. Barberà MJ, Puig I, Domínguez D, Julien-Grille S, Guaita-Esteruelas S, Peiró S, Baulida J, Francí C, Dedhar S, Larue L, García de Herreros A. Regulation of Snail transcription during epithelial to mesenchymal transition of tumor cells. Oncogene 2004;23:7345-54.
35. Tiwari N, Gheldof A, Tatari M, Christofori G. EMT as the ultimate survival mechanism of cancer cells. Semin Cancer Biol 2012;22:194-207.
36. Schmalhofer O, Brabletz S, Brabletz T. E-cadherin, beta-catenin, and ZEB1 in malignant progression of cancer. Cancer Metastasis Rev 2009;28:151-66.
37. Jin H, Yu Y, Zhang T, Zhou X, Zhou J, Jia L, Wu Y, Zhou BP, Feng Y. Snail is critical for tumor growth and metastasis of ovarian carcinoma. Int J Cancer 2010;126:2102-11
38. Kuijper S, Beverdam A, Kroon C, Brouwer A, Candille S, Barsh G, Meijlink F. Genetics of shoulder girdle formation: roles of Tbx15 and aristaless-like genes. Development 2005;132:1601-10.
39. Sharma T, Ettensohn CA. Activation of the skeletogenic gene regulatory network in the early sea urchin embryo. Development 2010;137:1149-57.
40. Wu SY, Yang YP, McClay DR. Twist is an essential regulator of the skeletogenic gene regulatory network in the sea urchin embryo. Dev Biol 2008;319:406-15.
41. Capellini TD, Vaccari G, Ferretti E, Fantini S, He M, Pellegrini M, Quintana L, Di Giacomo G, Sharpe J, Selleri L, Zappavigna V. Scapula development is governed by genetic interactions of Pbx1 with its family members and with Emx2 via their cooperative control of Alx1. Development 2010;137:2559-69.

42. Twigg SR, Versnel SL, Nürnberg G, Lees MM, Bhat M, Hammond P, Hennekam RC, Hoogeboom AJ, Hurst JA, Johnson D, Robinson AA, Scambler PJ, Gerrelli D, Nürnberg P, Mathijssen IM, Wilkie AO. Frontorhiny, a distinctive presentation of frontonasal dysplasia caused by recessive mutations in the ALX3 homeobox gene. Am J Hum Genet 2009;84:698-705.

43. Kayserili H, Uz E, Niessen C, Vargel I, Alanay Y, Tuncbilek G, Yigit G, Uyguner O, Candan S, Okur H, Kaygin S, Balci S, Mavili E, Alikasifoglu M, Haase I, Wollnik B, Akarsu NA. ALX4 dysfunction disrupts craniofacial and epidermal development. Hum Mol Genet 2009;18:4357-66.

Figure legends

Figure 1. Depletion of ALX1 induces reversion of EMT. (A) The relative expression of ALX1 mRNA normalized to GAPDH mRNA in ovarian cancer cell lines was examined by quantitative RT-PCR. (B) Expression of ALX1 mRNA in ovarian cancer tissues were examined by in situ hybridization. Semiquantitative scoring of the image intensity was performed, and the association of ALX1 expression with tumor stage was determined. $P<0.05$ is considered to be significant. Representative images of stage I, stage II, stage III are shown. (C) Cells were transfected with control or ALX1 siRNA and pictures were taken after 72 h to visualize cellular morphology (Scale bar = 50 μm). (D) Cells were cultured on glass coverslips and transfected with siRNA. After 72 h, cells were fixed and immunostained with an anti-E-cadherin antibody and DAPI. (Green: E-cadherin, Blue: DAPI, Scale bar = 50 μm). (E) Total RNA was extracted from siRNA-transfected cells and the mRNA expression levels of the indicated genes were determined by RT-PCR. (F)

Following siRNA transfection, the expression of the indicated proteins was examined by immunoblot.

Figure 2. ALX1 is required for cell invasion and the anchorage-independent growth of ovarian cancer cells. (A) Cells were transfected with siRNA and then subjected to the in vitro invasion assay 72 h later. Representative images of invading cells are shown (Scale bar = 30 μm). The graph indicates the average number of invaded cells per field. Three independent experiments were performed and the data are shown as the mean ± SD (**P<0.01). (B) Cells were transfected with siRNA and then subjected to the soft agar colony formation assay. The graph indicates the average number of colonies per field. Three independent experiments were performed and data are shown as the mean ± SD (**P<0.01). (C) SKOV3 cells constitutively expressing either control or ALX1 shRNA were generated and the expression levels of mRNA and protein were examined by RT-PCR or immunoblot for the indicated genes. (D) ShCtrl and shALX1 SKOV3 cells were subcutaneously injected into the femurs of mice and tumor volume was measured. The graph shows the average volume of six tumors from each cell line (*P<0.05). (E) Thirty-six days after tumor injection, mice were sacrificed and tumor weight was measured. The picture shows the extracted tumors and the graph indicates the average tumor weight from the six tumors derived from each cell line (*P<0.05) (Scale bar = 2 cm).

Figure 3. Exogenous expression of ALX1 in SKOV3 cells promotes EMT, cell invasion and anchorage-independent growth. (A) Structures of full-length and mutant ALX1. (B) SKOV3 cells constitutively expressing GFP (GFP), GFP-tagged full length ALX1 (FL),

or GFP-tagged ALX1 deleted of either the homeodomain (Δhomeo) or the OAR domain (ΔOAR) were generated by retroviral infection. The pictures are representative images showing the cellular morphology of each cell line (Scale bar = 50 μm). (C) The expression of the indicated proteins from each cell line was examined by immunoblot. (D) The invasive properties of each cell line were evaluated using an in vitro invasion assay. The graph shows the average number of invaded cells per field. Three independent experiments were performed and the data are represented as the mean ± SD (** P<0.01, * P<0.05). (E) Each cell line was subjected to a soft agar colony formation assay. The average number of colonies per field is indicated in the graph. Three independent experiments were performed and the data are presented as the mean ± SD (** P<0.01, * P<0.05).

Figure 4. Exogenous expression of ALX1 in MCF10A cells induces EMT. (A) The pictures are representative images showing the cellular morphology of the indicated cell lines (Scale bar = 50 μm). (B) Cells were cultured on glass coverslips and then fixed and immunostained with an anti-E-cadherin antibody and DAPI. (Scale bar = 50 μm). (C). Cells were cultured on glass coverslips and then fixed and immunostained with rhodamine-conjugated phalloidin and an anti-vinculin antibody. The nucleus was stained by DAPI (Scale bar = 50 μm). (D) Cells were lysed and the expression of the indicated proteins was analyzed by immunoblot. (E) GFP and FL MCF10A cells were subjected to in vitro migration assay. The graph shows the average number of migrated cells per field. Three independent experiments were performed and the data are represented as the mean ± SD (** P<0.01). (F) GFP and FL MCF10A cells were subjected to in vitro invasion assay. The graph shows the average number of invaded cells per

field. Three independent experiments were performed and the data are represented as the mean ± SD (**P<0.01).

Figure 5. Snail expression is regulated by ALX1. (A) Seventy-two hours after transfection with siRNA, total RNA was extracted to examine changes in the mRNA expression levels of the indicated genes. (B) The expression of Snail in siRNA-transfected cells was examined by immunoblot. (C) SKOV3 cells cultured on glass coverslips were transfected with siRNA and after 72 h, cells were fixed and immunostained for E-cadherin and Snail. The nucleus was visualized using DAPI (Scale bar = 50 μm). (D) The expression of Snail in the indicated cell lines was examined by immunoblot. (E) 293T cells were co-transfected with the ALX1 expression vector together with the pGL4-Snail/promoter and pRK-Luc expression vectors. Three independent experiments were performed and the relative luciferase activity is indicated (**P<0.01). (F) SKOV3 cells were transfected with ALX1-targeting siRNAs together with the pGL4-Snail/promoter and pRK-Luc vectors. After 72 h, luciferase activity was measured. Three independent experiments were performed and the relative luciferase activity is indicated (**P<0.01). (G) The relative expression of ALX1, Snail and Slug mRNA normalized to GAPDH mRNA in 19 cancer tissues was determined by quantitative RT-PCR. The Pearson's correlation coefficients (r) are shown. Details of patients' samples are described in supplementary table 1.

Figure 6. Snail expression is required for ALX1-mediated EMT and cell invasion. (A) MCF10A cells constitutively expressing GFP-ALX1 were transfected with control or Snail siRNA. After 72 h, cells were fixed and immunostained for E-cadherin. The

nucleus was visualized with DAPI (Scale bar = 50 μm). (B) Cells were transfected with siRNA and the expression of the indicated proteins was analyzed by immunoblot. (C) SKOV3 cells constitutively expressing GFP or GFP-ALX1 were transfected with control or Snail-targeting siRNA. After 72 h, the expression of the indicated proteins was examined by immunoblot. (D) Cells were transfected with siRNA and then subjected to an in vitro invasion assay. The graph shows the average number of invaded cells per field. Three independent experiments were performed and the data are presented as the mean ± SD (**P<0.01). (E) SKOV3 cells constitutively expressing GFP-Snail were transfected with siRNA and the expression of the indicated proteins was analyzed by immunoblot. (F) Cells were transfected with siRNA and then subjected to an invasion assay 72 h later. The graph shows the average number of invaded cells per field. Three independent experiments were performed, and the data are presented as the mean ± SD (n.s., not significant).

Author Manuscript Published OnlineFirst on January 3, 2013; DOI: 10.1158/0008-5472.CAN-12-2377
Author manuscripts have been peer reviewed and accepted for publication but have not yet been edited.

Fig. 1

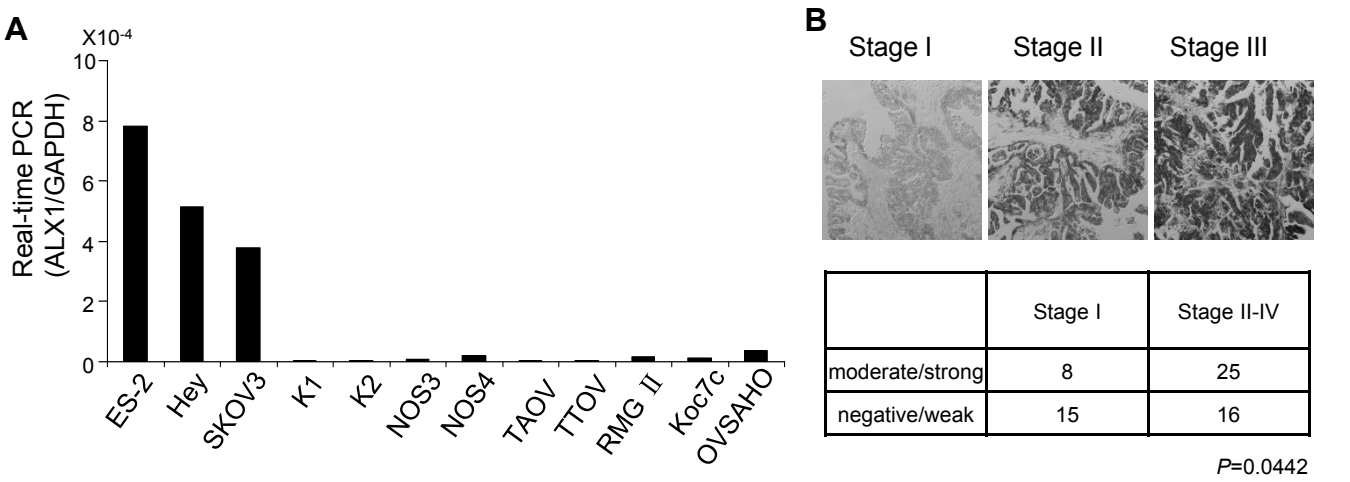

	Stage I	Stage II-IV
moderate/strong	8	25
negative/weak	15	16

P=0.0442

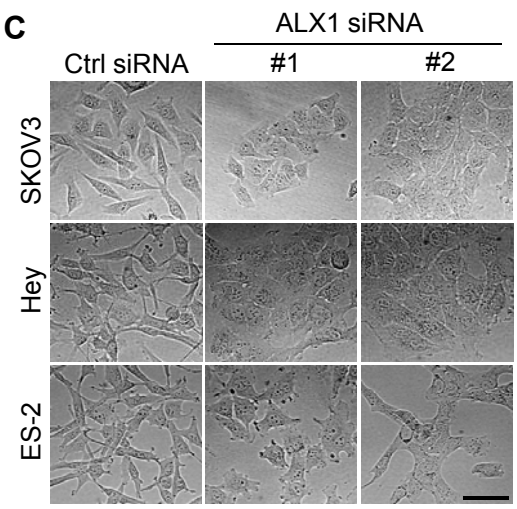

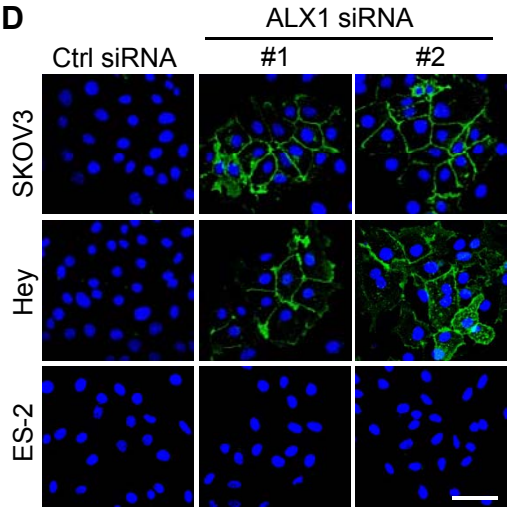

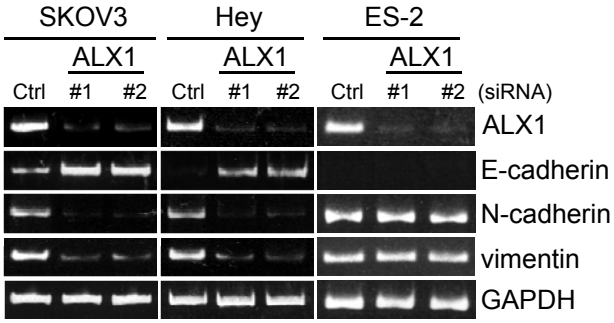

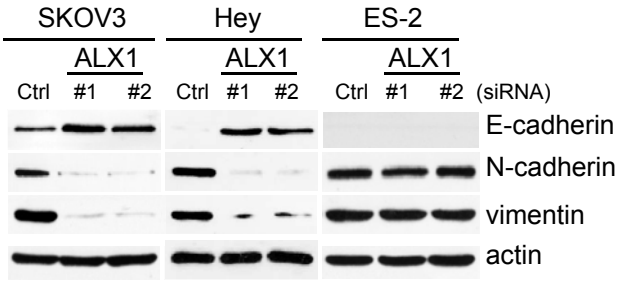

Author Manuscript Published OnlineFirst on January 3, 2013; DOI: 10.1158/0008-5472.CAN-12-2377
Author manuscripts have been peer reviewed and accepted for publication but have not yet been edited.

Fig. 2

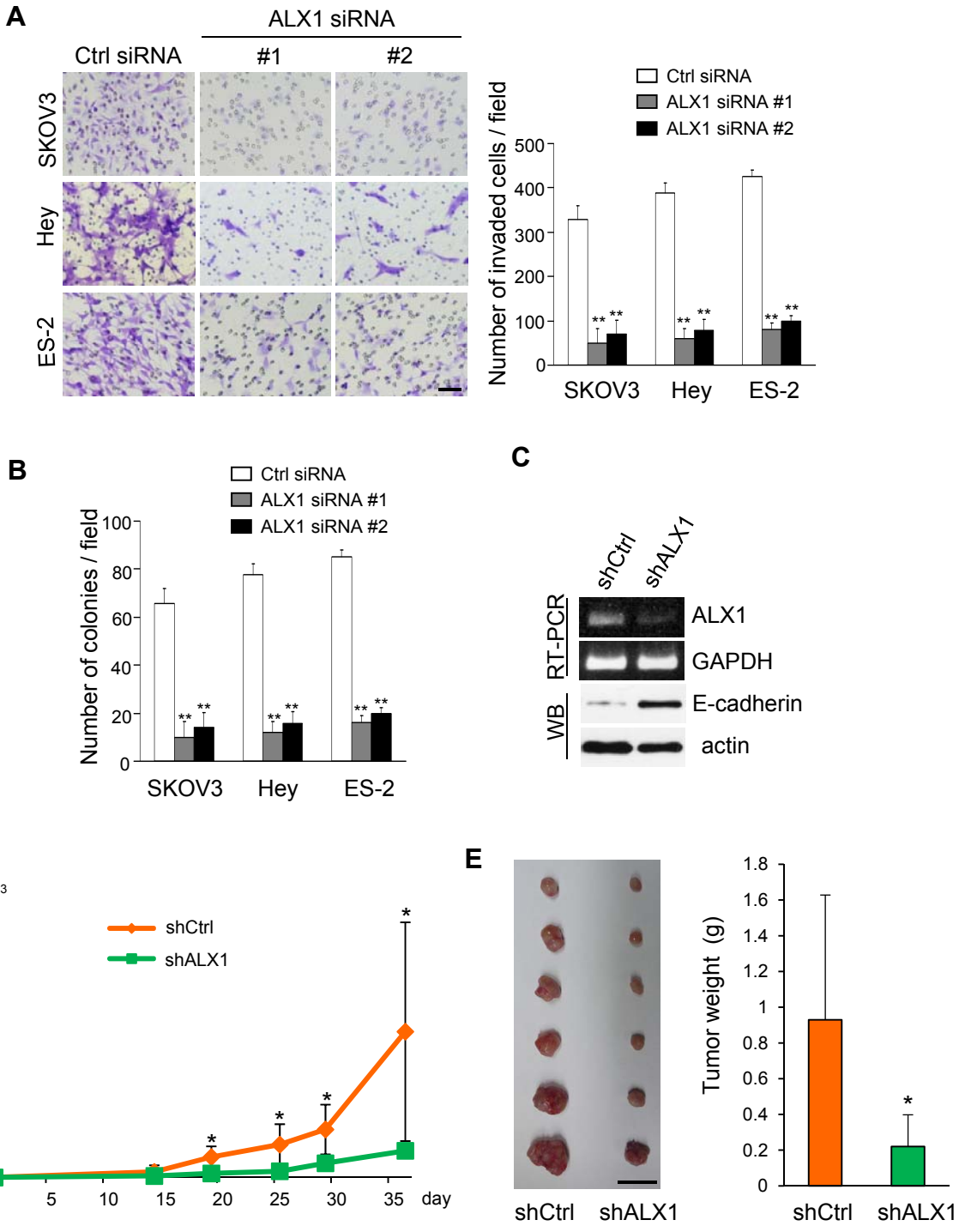

Fig. 3

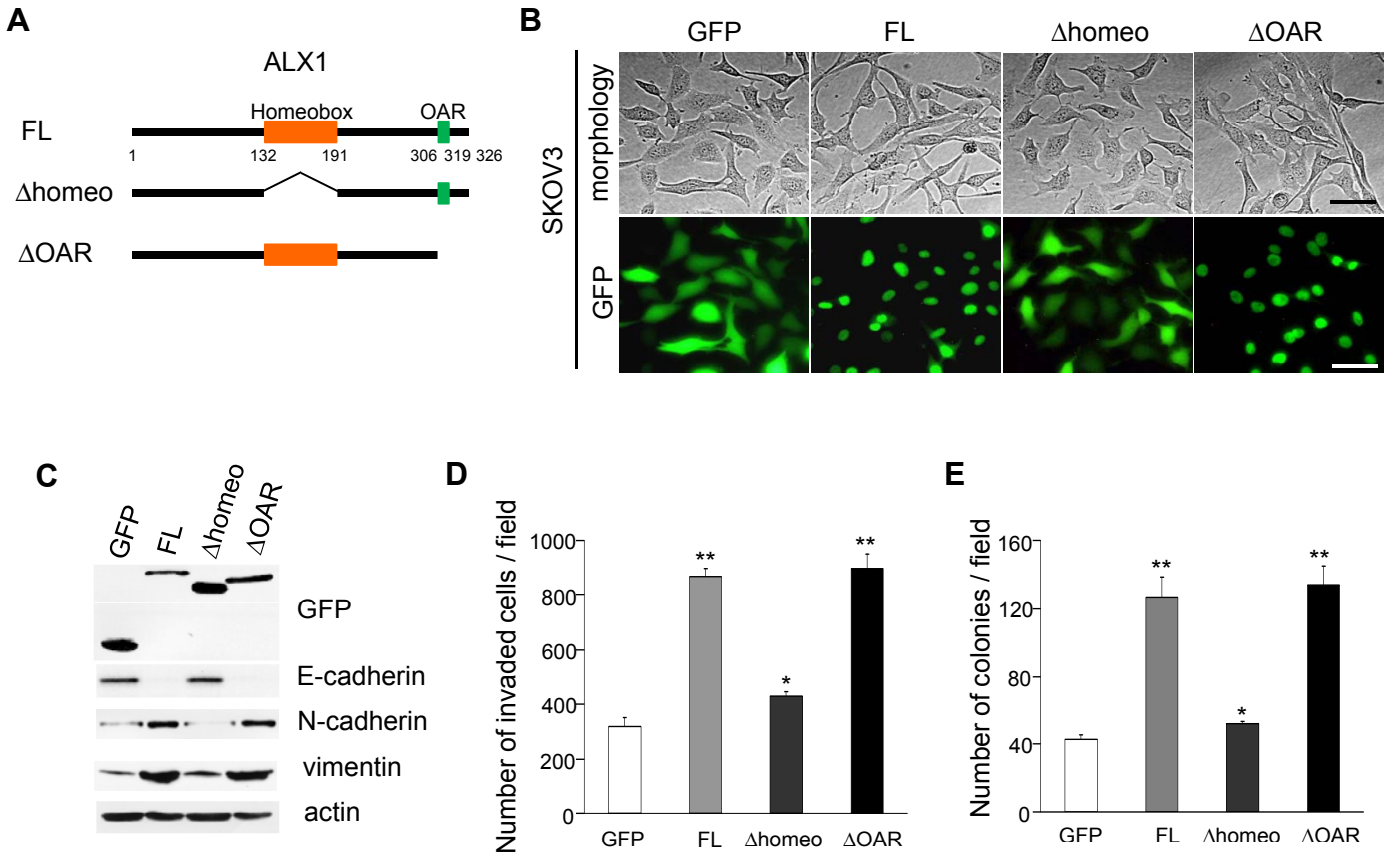

Author Manuscript Published OnlineFirst on January 3, 2013; DOI: 10.1158/0008-5472.CAN-12-2377
Author manuscripts have been peer reviewed and accepted for publication but have not yet been edited.

Fig 4

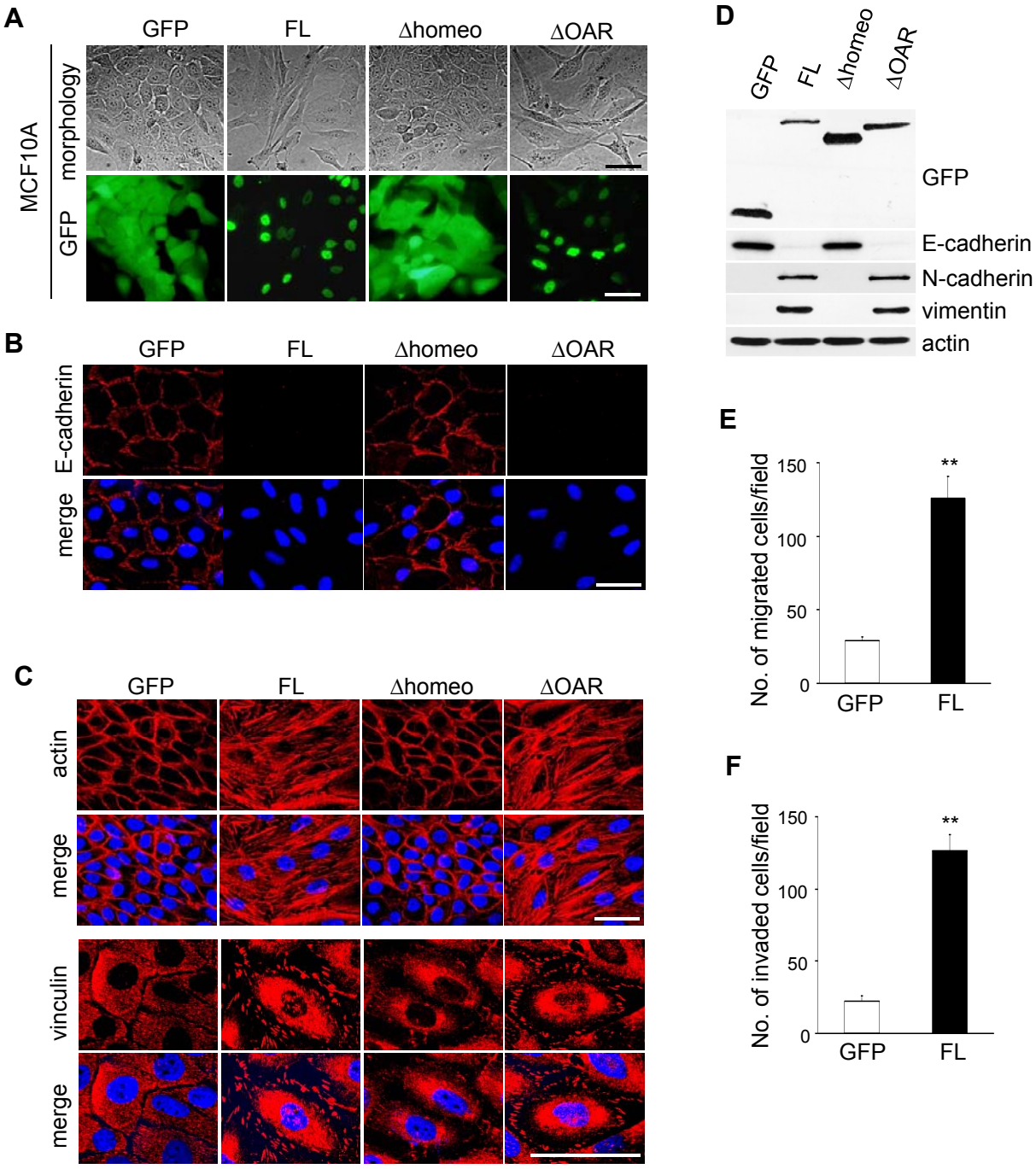

Author Manuscript Published OnlineFirst on January 3, 2013; DOI: 10.1158/0008-5472.CAN-12-2377
Author manuscripts have been peer reviewed and accepted for publication but have not yet been edited.

Fig5

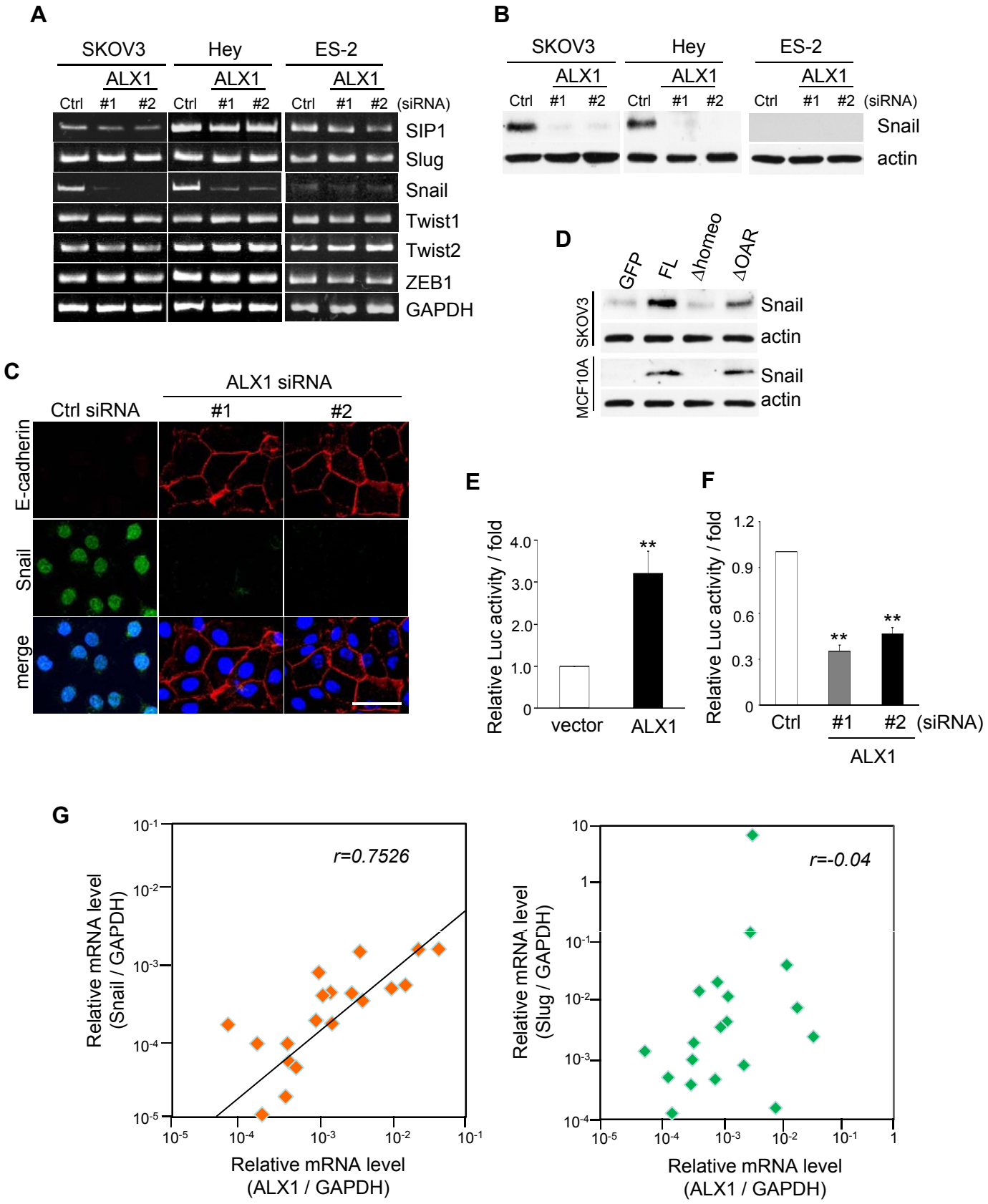

Author Manuscript Published OnlineFirst on January 3, 2013; DOI: 10.1158/0008-5472.CAN-12-2377
Author manuscripts have been peer reviewed and accepted for publication but have not yet been edited.

Fig6

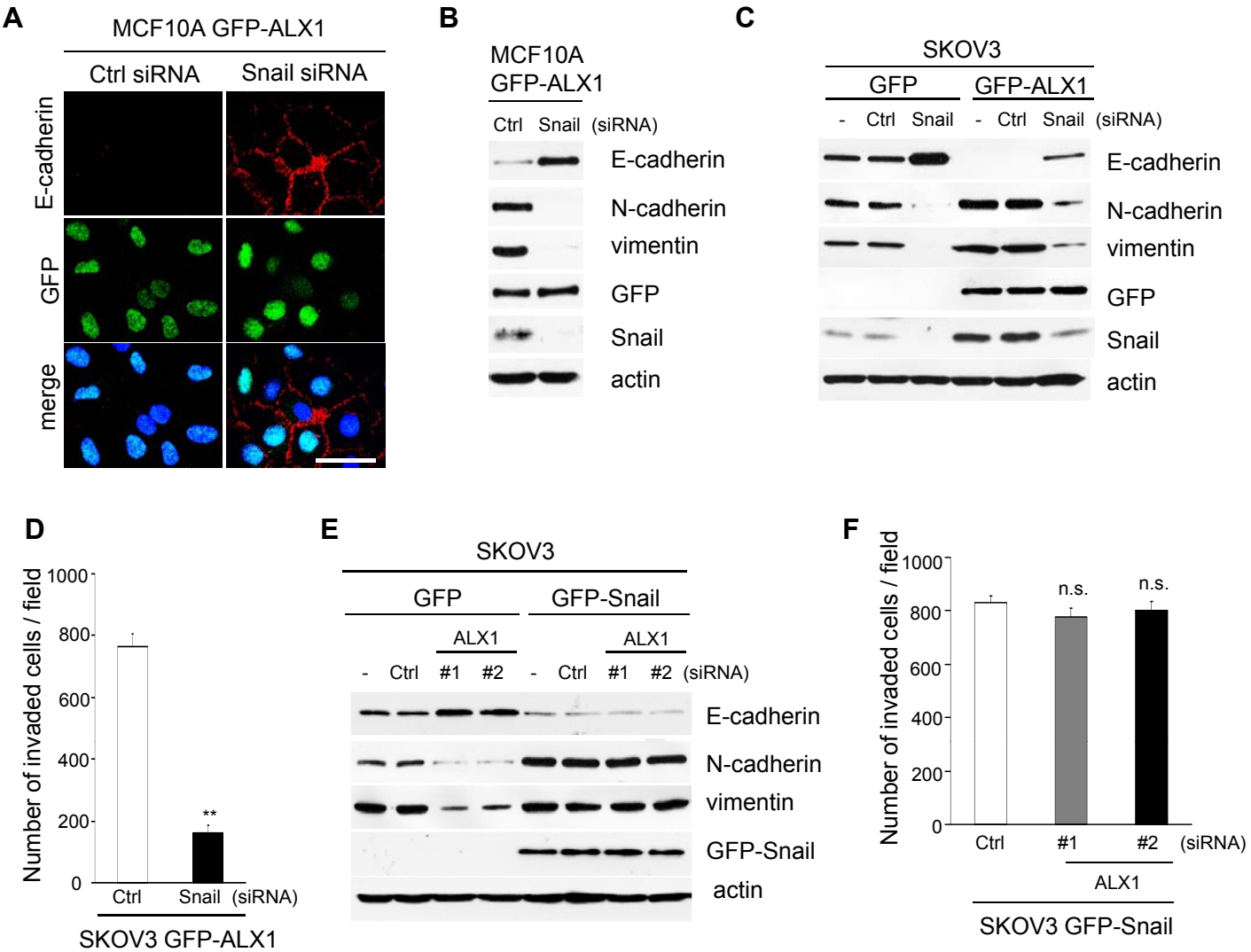

Cancer Research
The Journal of Cancer Research (1916–1930) | The American Journal of Cancer (1931–1940)

AACR American Association for Cancer Research

ALX1 induces Snail expression to promote epithelial to mesenchymal transition and invasion of ovarian cancer cells

Hong Yuan, Hiroaki Kajiyama, Satoko Ito, et al.

Cancer Res Published OnlineFirst January 3, 2013.